Curium(III) Radiation-Induced Reaction Kinetics in Aqueous Media

Journal:	*Dalton Transactions*
Manuscript ID	DT-ART-04-2021-001268.R1
Article Type:	Paper
Date Submitted by the Author:	13-Jul-2021
Complete List of Authors:	Horne, Gregory; Idaho National Laboratory, Center for Radiation Chemistry Research Grimes, Travis; Idaho National Laboratory, Aqueous Separations and Radiochemistry Zalupski, Peter; Idaho National Laboratory, Aqueous Separations and Radiochemistry Meeker, David; Idaho National Laboratory, Center for Radiation Chemistry Research; Florida State University, Department of Chemistry & Biochemistry Albrecht-Schoenzart, Thomas; Florida State University, Chemistry and Biochemistry Cook, Andrew; Brookhaven National Laboratory, Chemistry Department Mezyk, Stephen; California State University at Long Beach, Chemistry and Biochemistry

ARTICLE

Curium(III) Radiation-Induced Reaction Kinetics in Aqueous Media

Gregory P. Horne[a]*, Travis S. Grimes[a], Peter R. Zalupski[a], David S. Meeker[a,b], Thomas E. Albrecht-Schönzart[b], Andrew R. Cook[c], and Stephen P. Mezyk[d]*.

Received 00th April 2021,
Accepted 00th July 2021

DOI: 10.1039/x0xx00000x

Insight into the effects of radiolytic processes on the actinides is critical for advancing our understanding of their solution chemistry because the behaviour of these elements cannot be easily separated from the influence of their inherent radiation field. However, minimal information exists on the radiation-induced redox behaviour of curium (Cm), a key trivalent transuranic element present in used nuclear fuel and frequently used as an alpha radiation source. Here we present a kinetic study on the aqueous redox reactions of Cm(III) with radicals generated through the radiolysis of aqueous media. In particular, we probe reaction kinetics in nitric acid solutions that are used as the aqueous phase component of used nuclear fuel reprocessing solvent systems. Second-order rate coefficients (k) were measured for the reaction of Cm(III) with the hydrated electron (e_{aq}^-, $k = (1.25 \pm 0.03) \times 10^{10}$ M^{-1} s^{-1}), hydrogen atom ($H^\bullet$, $k = (5.16 \pm 0.37) \times 10^{8}$ M^{-1} s^{-1}), hydroxyl radical ($^\bullet OH$, $k = (1.69 \pm 0.24) \times 10^{9}$ M^{-1} s^{-1}), and nitrate radical ($NO_3^\bullet$, $k = (4.83 \pm 0.09) \times 10^{7}$ M^{-1} s^{-1}). Furthermore, the first-ever Cm(II) absorption spectrum (300-700 nm) is also reported. These kinetic data dispel the status quo notion of Cm(III) possessing little to no redox chemistry in aqueous solution, and suggest that the resulting Cm(II) and Cm(IV) transients could exist in irradiated aqueous solutions and be available to undergo subsequent redox chemistry with other solutes.

Introduction

One of the main goals behind reprocessing used nuclear fuel (UNF) is to minimise the heat load and radiotoxicity for the long-term storage of spent nuclear fuel (SNF) in a geological repository. This challenge necessitates the recovery of the heavier transplutonium actinide elements that are typically long-lived alpha-radiation emitters. Their removal by multi-recycle strategies can reduce the radiotoxic lifetime of SNF from 300,000 years to just 400 years.[1] However, recovery of the trivalent transuranic elements, notably, americium (Am) and curium (Cm), is complicated by their chemical similarities to the trivalent lanthanides (Ln) present in far larger amounts from fuel fission events.[2-5] Consequently, a significant research effort has been devoted to the development of trivalent *f*-element separation technologies, especially using solvent extraction.[6-14]

In addition, the effects of ionizing radiation on the chemical components of these extraction systems have been, and continue to be, investigated.[15-20] However, the majority of these studies have overlooked the role of the actinide elements themselves. Many of these elements have already been shown to influence the suite of available radiolysis products through chemical reactions,[21-23] and by undergoing radiation-induced redox chemistry[24-26] that ultimately affects the radiation robustness and performance of a given reprocessing technology.

The inherent multi-component (predominantly alpha, beta, and gamma) radiation field present in UNF loaded reprocessing solvent induces metal ion and extraction ligand radiolysis. In aqueous environments the actinide ions are more available for direct reaction with the radiolysis radical species produced from the aqueous phase constituents, which are predominantly water, nitrate ions (NO_3^-), and nitric acid (HNO_3):[27, 28]

$$H_2O \rightsquigarrow e_{aq}^-, H^\bullet, {}^\bullet OH, H_2O_2, H_2, H_{aq}^+, \qquad (1)$$

$$NO_3^-/HNO_3 \rightsquigarrow e^-, NO_3^\bullet, NO_2^-/HNO_2, O, H_{aq}^+. \qquad (2)$$

Many of these aqueous phase radiolytic species have already been shown to dictate the oxidation state distribution of actinides under envisioned reprocessing conditions, e.g., for neptunium (Np) and oxidized Am.[24-26] This is important chemistry, as the oxidation state of these actinides controls their distribution between the aqueous and organic phases. In contrast, there is minimal information available for the radiolytically-induced redox behaviour of Cm, despite Cm isotopes being frequently used as an internal radiation source to investigate the effects of alpha (α-) particles on both applied and fundamental systems.[29-32] While the measured redox behaviour of Cm ions (Fig. 1) suggests that Cm(III) is the only state present in acidic aqueous solution,[33] Sullivan and co-workers,[34] using picosecond pulsed electron radiolysis techniques coupled with nanosecond spectroscopic time resolution, reported that Cm(III) is susceptible to reduction by the hydrated electron (e_{aq}^-, $E^o = -2.9$ V)[27] and also oxidation by the hydroxyl radical ($^\bullet OH$, $E^o = 2.7$ V)[27]:

---

[a] Idaho National Laboratory, Center for Radiation Chemistry Research, Idaho Falls, ID, P.O. Box 1625, 83415, USA
[b] Florida State University, Department of Chemistry and Biochemistry, Tallahassee, FL 32306, USA.
[c] Department of Chemistry, Brookhaven National Laboratory, Upton, New York, 11973, USA.
[d] Department of Chemistry and Biochemistry, California State University Long Beach, 1250 Bellflower Boulevard, Long Beach California, 90840-9507, USA.
*E-mail: gregory.p.horne@inl.gov and stephen.mezyk@csulb.edu.

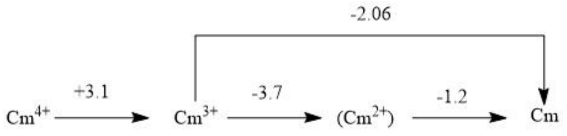

Fig. 1. Summary of redox potentials (V) for Cm ions in acidic solution.

$$Cm^{3+} + e_{aq}^{-} \rightarrow Cm^{2+} \qquad \tau_{1/2}(Cm^{2+}) = 1.2 \times 10^{-5}\ s \quad (3)$$

$$Cm^{2+} (+ H_2O) \rightarrow Cm^{3+} \qquad k \sim 6 \times 10^{4}\ s^{-1} \quad (4)$$ [21]

$$Cm^{3+} + {}^{\bullet}OH \rightarrow Cm^{4+} + OH^{-} \qquad \tau_{1/2}(Cm^{4+}) = 2.0 \times 10^{-5}\ s \quad (5)$$

$$Cm^{4+} (+ H_2O) \rightarrow Cm^{3+} \qquad k \sim 3 \times 10^{4}\ s^{-1}. \quad (6)$$ [21]

Even higher oxidation states, notably Cm(VII), have been proposed to form in cold, basic, aqueous solutions through the reactions of oxide ($O^{\bullet-}$, the deprotonated form of $^{\bullet}OH$) and carbonate ($CO_3^{\bullet-}$) radicals.[35] However, assignment of these radical driven processes and the corresponding approximate half-life ($\tau_{1/2}$) values have been based only on observations of the growth and decay of UV-visible spectral transients, attributed to Cm(II) and Cm(IV) transients. No direct, or competition kinetics based, measurements have been made for the instigating radicals, i.e., e_{aq}^{-} and $^{\bullet}OH$. Consequently, there are no available absolute rate coefficients (k) for these processes, and yet they are essential for the development of computer models for the prediction of Cm behaviour in radiation fields under envisioned reprocessing conditions. A similar understanding is necessary for predicting Cm speciation under SNF storage conditions,[36] and its physiological uptake in the event of an accidental release of radiological/nuclear material into the environment.[37]

Furthermore, the reactions of both the hydrogen atom ($H^{\bullet}$, $E^{o} = -2.3$ V)[27] and nitrate radical ($NO_3^{\bullet}$, $E^{o} = 2.3 - 2.6$ V)[38] are arguably more important under recycling conditions because they are preferentially formed under the concentrated HNO_3 solution conditions employed by reprocessing solvent systems:

$$H_{aq}^{+} + e_{aq}^{-} \rightarrow H^{\bullet} \qquad k = 2.3 \times 10^{10}\ M^{-1}\,s^{-1} \quad (7)$$ [27]

$$HNO_3 + {}^{\bullet}OH \rightarrow {}^{\bullet}NO_3 + H_2O \qquad k = 1.9 \times 10^{7}\ M^{-1}\,s^{-1}. \quad (8)$$ [39]

Despite their importance there are no rate coefficients for their reaction with Cm(III).

Hence, to provide a comprehensive understanding for the radiolytic behaviour of Cm(III) under aqueous phase reprocessing conditions, we present a fundamental pulsed electron reaction kinetics study, wherein we report rate coefficients for the reaction of Cm(III) with radicals (e_{aq}^{-}, $H^{\bullet}$, $^{\bullet}OH$, and $NO_3^{\bullet}$) expected under advanced UNF reprocessing solvent system conditions from aqueous HNO_3 radiolysis.

Experimental

Caution! The curium-248 solutions employed in this work were highly radioactive. Handling was performed in dedicated radiological and nuclear facilities using well established radiological safety protocols.

Materials

Curium-248 (^{248}Cm, $\tau_{1/2} = 3.48 \times 10^{5}$ years, $E_{\alpha} = 5.16$ MeV) was sourced from on-hand oxide stocks at Idaho National Laboratory (INL). Nitric acid (HNO_3, *≥99.999% trace metals basis*), perchloric acid ($HClO_4$, *≥99.999% trace metals basis*), hydrochloric acid (HCl, *≥99.999% trace metals basis*), parachlorobenzoic acid (pCBA, *99%*), potassium thiocyanate (KSCN, ≥99.0% *ACS Reagent Grade*), and tertiary butanol (tBuOH, *≥99.5% anhydrous*) were obtained from MilliporeSigma (Burlington, MA, USA). Unless otherwise stated, all chemicals were used without further purification. Compressed nitrogen (N_2) and nitrous oxide (N_2O) were purchased from Airgas (Radnor, PA, USA) with purities ≥ 99.5%. Ultra-pure water (18.2 MΩ cm) was used to prepare all aqueous solutions.

Curium Purification

Prior to sample preparation, the Cm-248 stock required purification and metathesis into $HClO_4$ solution. The Cm(III) stock was acidified to ~6 M H_{aq}^{+} using concentrated HNO_3, and then run through an Eichrom normal resin diglycolamide (DGA) column. The coordinated Cm(III) on the column was then sequentially washed with 6.0 M HNO_3 and 8.0 M HCl before it was eluted with 20 mM HCl. Hydrochloric acid was distilled off via a series of evaporation cycles and the Cm(III) residue was dissolved in 10 mM $HClO_4$. The resulting Cm(III)/$HClO_4$ solution was analysed using a Cary 6000i UV-vis-NIR spectrophotometer (Agilent, Santa Clara, CA, USA) to determine the concentration of Cm(III) recovered (3.7 mM/0.0033 mg) by its absorption ($\lambda_{max} = 396$ nm, $\varepsilon = 52.9\ M^{-1}\ cm^{-1}$).[40] This Cm(III)/$HClO_4$ stock solution was used to prepare all subsequent samples for irradiation through serial dilution.

Pulsed Electron Irradiations

Reaction kinetics of Cm(III) with radicals (e_{aq}^{-}, $H^{\bullet}$, $^{\bullet}OH$, and $NO_3^{\bullet}$) expected under advanced UNF reprocessing solvent system conditions from aqueous HNO_3 radiolysis, were investigated using the picosecond pulsed electron radiolysis/transient absorption system at the Brookhaven National Laboratory (BNL) Laser Electron Accelerator Facility (LEAF).[41]

Samples comprised of varying concentrations of Cm(III) (≤ 0.27 mM) in aqueous solutions formulated to promote the formation of specific radicals and measurement of their associated reaction kinetics:

- *Hydrated Electron (e_{aq}^{-}).* N_2-saturated aqueous solutions of 0.18-0.72 mM $HClO_4$ and 0.4-0.5 M *t*BuOH. Direct decay kinetics of this transient were observed at 720 nm.
- *Hydrogen Atom ($H^{\bullet}$).* N_2-saturated aqueous solutions of 73-100 μM pCBA, 0.07-0.10 M $HClO_4$, and 10-20 mM tBuOH. Kinetics were determined using the change in growth rate of the [pCBA-$H^{\bullet}$] transient adduct absorbance directly observed at 365 nm.
- *Hydroxyl Radical ($^{\bullet}OH$).* N_2O-saturated aqueous solutions of 73-100 μM KSCN and 10 mM $HClO_4$. Competition kinetics with the $[SCN]_2^{\bullet-}$ transient observed at 470 nm.
- *Nitrate Radical ($NO_3^{\bullet}$).* N_2O-saturated aqueous solutions

of 4.5-6.0 M HNO_3. Direct decay kinetics observed at 630 nm.

Sample solutions were irradiated in 1.0 cm optical pathlength, screw-cap sealed, spectrosil quartz, semi-micro, Suprasil Starna Scientific Ltd. (Ilford, United Kingdom) cuvettes. Radical decay and growth kinetics were followed using an FND-100Q silicon diode detector, and digitized by a LeCroy WaveRunner 640Zi oscilloscope (4 GHz, 8 bit). Interference filters (~10 nm bandpass) were used for wavelength selection of the analysing light. Dosimetry was achieved using N_2O saturated solutions of 10 mM KSCN at $\lambda_{max} = 470$ nm ($G^*\varepsilon = 5.2 \times 10^{-4}$ m^2 J^{-1}).[42] Quoted errors for the presented second-order reaction rate coefficients (k) are a combination of measurement precision and sample concentration errors.

Results and Discussion

The measured second-order rate coefficients for the reaction of Cm(III) with e_{aq}^-, $H^\bullet$, $^\bullet OH$, and $NO_3^\bullet$ are summarized in Table 1.

Table 1. Summary of measured second-order rate coefficients for the reaction of aqueous Cm(III) with e_{aq}^-,$H^\bullet$, $^\bullet OH$, and $NO_3^\bullet$ at 25°C.

Radical Species	***k*** (M^{-1} s^{-1})
e_{aq}^-	$(1.25 \pm 0.03) \times 10^{10}$
$H^\bullet$	$(5.16 \pm 0.37) \times 10^8$
$^\bullet OH$	$(1.69 \pm 0.24) \times 10^9$
$NO_3^\bullet$	$(4.83 \pm 0.09) \times 10^7$

Hydrated Electron

Kinetics for the reaction of Cm(III) with e_{aq}^- (Eq. 3) are shown in Fig. 2. Increasing the concentration of Cm(III) in solution afforded a significant decrease in the lifetime of e_{aq}^-, as demonstrated by the e_{aq}^- decay traces shown in the inset of Fig. 1 (A). Scavenging of e_{aq}^- by Cm(III) was complemented by an observable ingrowth attributed to the Cm(II) product, the transient absorption spectrum for which is shown in Fig. 1 (A). This is the first-ever aqueous solution Cm(II) spectrum to be reported, and is consistent with having a λ_{max} value at < 240 nm, as previously presented by Sullivan and co-workers.[34] The corresponding pseudo first-order rate coefficients (k') for the reaction of Cm(III) with e_{aq}^- are given in Fig. 1 (B). These data facilitated calculation of the overall second-order rate coefficient given in Table 1, as $(1.25 \pm 0.03) \times 10^{10}$ M^{-1} s^{-1}. This value is essentially diffusion-limited in aqueous solution and significantly higher than rate coefficients reported for other trivalent actinide elements: $k_{Am(III)} = 1\text{-}3 \times 10^8$ M^{-1} s^{-1}, (E° = -2.3V); $k_{Cf(III)} > 3 \times 10^9$ M^{-1} s^{-1},[21] (E° = -1.60 V); and $k_{Bk(III)} = 1.12 \times 10^9$ M^{-1} s^{-1},[43] (E° = -2.8V). The fast reduction rate coefficient for Cm(III) is surprising considering there is a relatively small favourable difference between the redox potentials for the Cm(III)/Cm(II) couple (E° = -2.8 V)[44] and e_{aq}^- (E° = -2.9 V)[27]. Overall, these direct kinetic measurements support Sullivan and co-workers postulation that e_{aq}^- is capable of reducing Cm(III) to Cm(II), albeit transiently.[34]

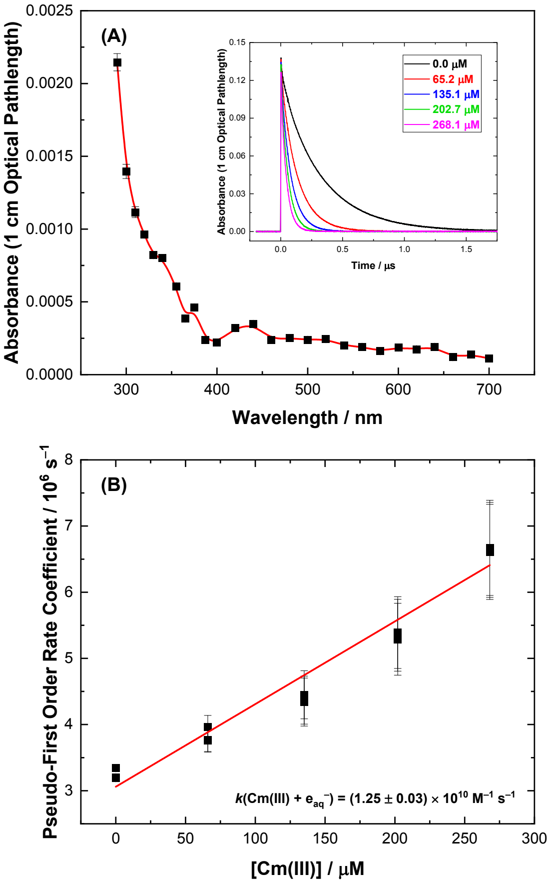

Fig. 2. **(A)** Transient absorption spectrum measured for Cm(II) at 0.5 μs after the pulse for 0.27 mM Cm(III) in N_2-saturated aqueous $HClO_4$/*t*BuOH solution. *Inset*: measured kinetic traces at 720 nm for pulsed electron irradiated N_2-saturated solutions of Cm(III) in $HClO_4$/*t*BuOH at room temperature. Kinetic data were analysed using a single-exponential decay function. **(B)** Second-order determination of the rate coefficient for the reaction of Cm(III) with e_{aq}^-. Pseudo-first-order values were corrected for contributions from the reaction of H_{aq}^+ with e_{aq}^-. The weighted linear fit corresponds to a reaction rate coefficient of $k(\text{Cm(III)} + e_{aq}^-) = (1.25 \pm 0.03) \times 10^{10}$ M^{-1} s^{-1}, $R^2 = 0.99$.

Despite this demonstration of the reduction of Cm(III) by e_{aq}^-, the extent of this reaction under envisioned UNF reprocessing conditions is expected to be small due to rapid scavenging of e_{aq}^- (and its precursor, e_{pre}^-) by H_{aq}^+ (Eq. 7 and 9) and NO_3^- (Eq. 10 and 11):

$H_{aq}^+ + e_{pre}^- \rightarrow H^\bullet$ $k = 2.18 \times 10^{12}$ M^{-1} s^{-1} [45] (9)

$NO_3^- + e_{pre}^- \rightarrow NO_3^{\bullet 2-}$ $k = 1.0 \times 10^{13}$ M^{-1} s^{-1} [45] (10)

$NO_3^- + e_{aq}^- \rightarrow NO_3^{\bullet 2-}$ $k = 9.7 \times 10^9$ M^{-1} s^{-1}.[27] (11)

Hydrogen Atom

The $H^\bullet$ is a major radiolytic species under the acidic aqueous phase conditions employed by UNF reprocessing solvent systems. Based on H_{aq}^+ and NO_3^- scavenging capacities ($k_s = k[H_{aq}^+/NO_3^-]$), 18% and 70% of the available yield of e_{pre}^- and e_{aq}^- are partitioned to H_{aq}^+ (Eq. 7 and 9), respectively. This affords a

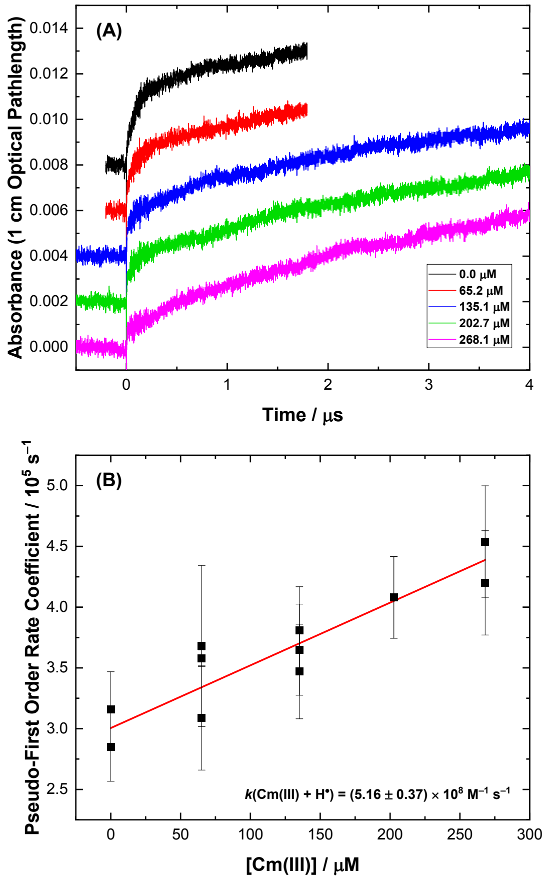

Fig. 3. **(A)** Measured kinetic traces of [pCBA-H•] at 365 nm for pulsed electron irradiated N_2-saturated solutions of Cm(III) in pCBA/$HClO_4$/*t*BuOH at room temperature. Kinetic data were analysed using a double-exponential growth function. **(B)** Second-order determination of the rate coefficient for the reaction of Cm(III) with H•. The weighted linear fit corresponds to a reaction rate coefficient of k(Cm(III) + H•) = (5.16 ± 0.37) × 10^8 M^{-1} s^{-1}, $R^2 = 0.99$.

significantly higher radiolytic yield – *G*-value – of H• (>0.06 µmol J^{-1})[27] compared to its value in water. Hydrogen atoms are ultimately partitioned between NO_3^- (Eq. 12), dissolved oxygen (O_2, Eq. 13), and UNF solutes, e.g., Cm(III) (Eq. 14):

$$NO_3^- + H^\bullet \rightarrow HNO_3^{\bullet -} \qquad k = 5.6 \times 10^6\ M^{-1}\ s^{-1} \tag{12}$$

$$O_2 + H^\bullet \rightarrow HO_2^\bullet \qquad k = 1.2 \times 10^{10}\ M^{-1}\ s^{-1} \tag{13}$$

$$Cm(III) + H^\bullet \rightarrow Cm(II) + H_{aq}^+. \tag{14}$$

Direct observation of H• decay was not possible with our wavelength range (290 to 1100 nm), as its $\lambda_{max} < 180$ nm.[46] Instead, kinetics were determined using pCBA as a probe molecule, where the increase in pseudo-first-order growth was measured as a function of added Cm(III) at constant pCBA concentration. These data are shown in Fig. 3. The pCBA probe reacts with H• (Eq. 15) to yield the corresponding adduct, [pCBA-H•], which grows in with an observable signal at a λ_{max} = 365 nm, as shown in Fig. 2 (A):

$$pCBA + H^\bullet \rightarrow [pCBA\text{-}H^\bullet] \qquad k = 2.5 \times 10^9\ M^{-1}\ s^{-1}.^{27} \tag{15}$$

As the concentration of Cm(III) increased, the growth rate of the [pCBA-H•] adduct correspondingly increases. Fitting these growths with a double-exponential growth function allow for calculation of the contribution of the pseudo first-order rate coefficients for Eq. 14 (from the slower exponential fit values), as given in Fig. 3 (B). From these values the overall second-order rate coefficient was then determined to be (5.16 ± 0.37) × 10^8 M^{-1} s^{-1}, Table 1. The rate of reaction for Cm(III) with H• is two orders of magnitude slower than the corresponding e_{aq}^- reduction process, which is typical for these two radical species.[27] Reduction of Cm(III) by H• was not expected to be as rapid as e_{pre}^-, as the redox potential for H• (E° = -2.3 V)[27] is much lower than the Cm(III)/Cm(II) couple (E° = -2.8 V)[44].

This H• atom rate coefficient is again much faster than reported for other trivalent actinides, $k_{Pu(III)} < 1 \times 10^6$ M^{-1} s^{-1} and $k_{Np(III)} = 6.3 \times 10^7$ M^{-1} s^{-1}.[43] Nevertheless, for the micromolar concentrations of Cm expected in UNF,[47] the competitive reduction of Cm(III) (*vs.* O_2 and NO_3^-) by H• atoms under reprocessing conditions is not expected to play a significant role.

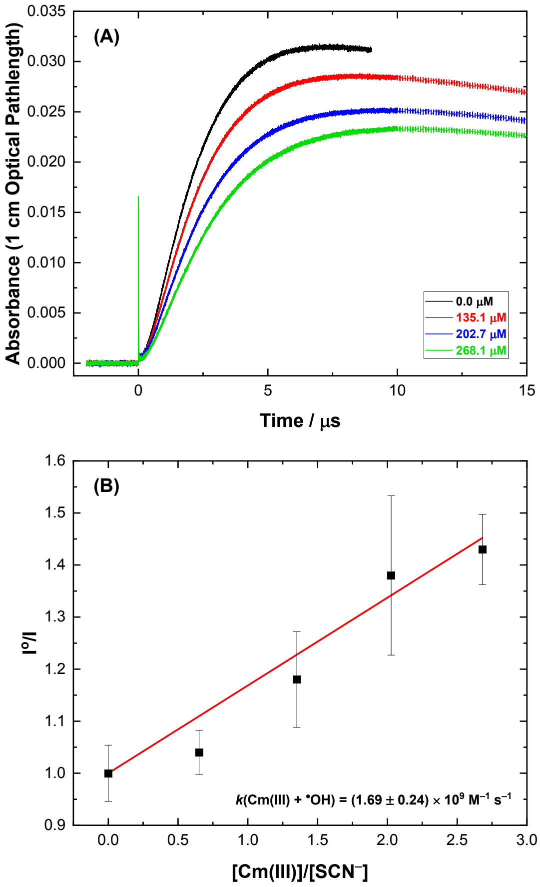

Fig. 4. **(A)** Measured kinetic traces of $[SCN]_2^{\bullet -}$ at 472 nm for pulsed electron irradiated N_2O-saturated solutions of Cm(III) in KSCN/$HClO_4$ at room temperature. Kinetic data were analysed using a single-exponential growth function. **(B)** Second-order determination of the rate coefficient for the reaction of Cm(III) with •OH. The weighted linear fit corresponds to a reaction rate coefficient of k(Cm(III) + •OH) = (1.69 ± 0.24) × 10^9 M^{-1} s^{-1}, $R^2 = 0.99$.

Hydroxyl Radical

As the transient Cm(IV) absorption spectrum also has a λ_{max} = 260 nm, the rate of reaction for Cm(III) with the $^{\bullet}OH$ radical (Eq. 5) was determined by competition kinetics, using SCN^- as the probe.[27] However, relative growth rates could not be used here, as the probe's measurable transient, $[SCN]_2^{\bullet-}$, is a secondary product:

$$SCN^- + {}^{\bullet}OH \rightarrow HOSCN^{\bullet-} \qquad k = 1.1 \times 10^{10}\ M^{-1}\ s^{-1}\ 27 \quad (16)$$

$$SCN^- + HOSCN^{\bullet-} \rightarrow [SCN]_2^{\bullet-} + OH^-. \qquad (17)$$

The relatively small complexation constants (β) for $Cm(SCN)_x$ species formation (β_1 = 1.53 and β_2 = 4.08)[48,49] indicate that the concentrations of such Cm species were negligible under our experimental conditions. The relative changes in the absorption intensity of $[SCN]_2^{\bullet-}$ as measured at λ_{max} = 470 nm, are shown in Fig. 4. (A). The $^{\bullet}OH$ radical competition between the Cm(III) and SCN^- reactions was then integrated to given the following analytical expression:

$$\frac{Abso}{Abs} = 1 + \frac{k\mathrm{Cm}[Cm(III)]}{k\mathrm{SCN}\text{-}\,[SCN-]}, \qquad (18)$$

where Abs° is the transient absorption maximum for $[SCN]_2^{\bullet-}$ in the absence of Cm(III), and Abs is the reduced transient absorption when Cm(III) is present. The ratio of k_{Cm}/k_{SCN^-} was obtained by plotting the ratios Abs°/Abs vs. [Cm(III)]/[SCN^-], from which the second-order rate coefficient (k_{Cm}) can be readily calculated, as shown in Fig. 3 (B). The rate of reaction for Cm(III) with $^{\bullet}OH$ was found to be (1.69 ± 0.24) × $10^9\ M^{-1}\ s^{-1}$, Table 1. This value is slightly slower than expected for a diffusion-controlled reaction, however, it is consistent with rate coefficients measured for other trivalent actinides: $k_{U(III)}$ = 4.1 × $10^8\ M^{-1}\ s^{-1}$;[21] $k_{Np(III)}$ = 0.3-1.6 × $10^9\ M^{-1}\ s^{-1}$;[22] $k_{Pu(III)}$ = 4.2 × $10^8\ M^{-1}\ s^{-1}$;[21] and $k_{Am(III)}$ = 0.3-1.6 × $10^9\ M^{-1}\ s^{-1}$.[21,22] Isolation of the transient Cm(IV) absorption spectrum was not possible, as the absorption band for $[SCN]_2^{\bullet-}$ is too broad.[46] However, the Cm(IV) spectra was previously determined by Keenan for Cm(IV) in 15 M CsF[50] but showed only minimal (ε < 50 $M^{-1}\ cm^{-1}$) absorption above 300 nm. Interestingly, the Cm(III)/Cm(IV) redox potential is -3.1 V,[51] which is larger than that for $^{\bullet}OH$ (E° = 2.7 V)[27].

In summary, the presented reaction kinetics for the oxidation of Cm(III) by $^{\bullet}OH$ support observations made by Sullivan and co-workers.[34] Further, the relatively fast rate of this process suggests that Cm(III) oxidation, and subsequent Cm(IV) redox chemistry, may play a significant role under UNF reprocessing conditions, especially for lower HNO_3 concentrations where $^{\bullet}OH$ is the prevalent oxidant.

Nitrate Radical

For high concentrations of HNO_3 (>1.0 M), $NO_3^{\bullet}$ is the dominant oxidising radical due to a combination of direct radiolysis (Eq. 2) and $^{\bullet}OH$ scavenging (Eq. 8). Kinetics for the reaction of Cm(III) with $NO_3^{\bullet}$ (Eq. 19) are shown in Fig. 5, and were performed by direct measurement of $NO_3^{\bullet}$ decay at 630 nm.

$$Cm^{3+} + NO_3^{\bullet} \rightarrow Cm^{4+} + NO_3^-. \qquad (19)$$

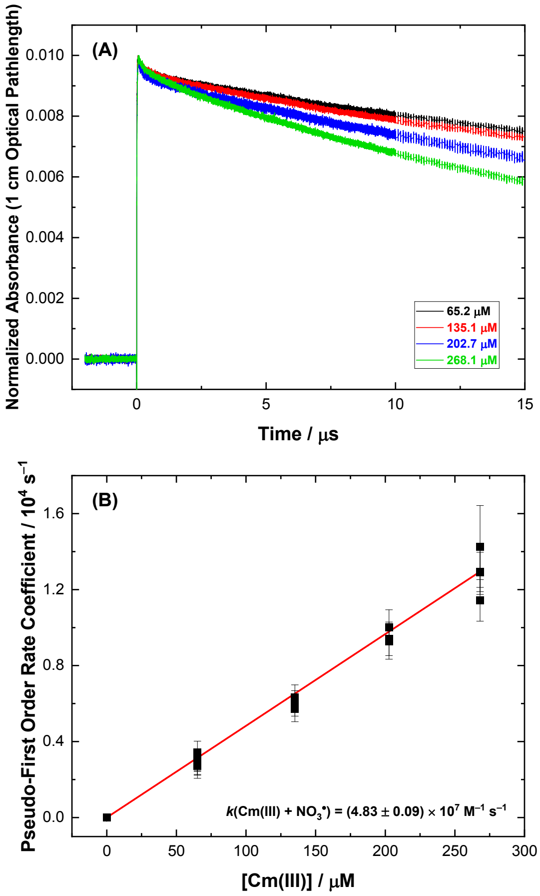

Fig. 5. (A) Measured kinetic traces of $NO_3^{\bullet}$ at 630 nm for pulsed electron irradiated N_2O-saturated solutions of Cm(III) in HNO_3 at room temperature. Kinetic data were analysed using a mixed (first- and second-order) decay function. **(B)** Second-order determination of the rate coefficient for the reaction of Cm(III) with $NO_3^{\bullet}$. The weighted linear fit corresponds to a reaction rate coefficient of $k(Cm(III) + NO_3^{\bullet})$ = (4.83 ± 0.09) × $10^7\ M^{-1}\ s^{-1}$, R^2 = 0.99.

These kinetic data were fit to a mixed (first- and second-order) decay expression, with the first-order component plotted in Fig. 5 (B). The rate of this oxidation process, $k(Cm(III) + NO_3^{\bullet})$ = (4.83 ± 0.09) × $10^7\ M^{-1}\ s^{-1}$, is two orders of magnitude slower than for the corresponding $^{\bullet}OH$ reaction, see Table 1. Our value is slower than the only other reported trivalent actinide value for Pu(III), $k_{Pu(III)}$ = 2.5 × $10^8\ M^{-1}\ s^{-1}$.[43] Such slow reactivity is in keeping with their respective redox potentials and typical trends in reaction behaviour.[27,52] However, despite the lower rate coefficient for the $NO_3^{\bullet}$ reaction, its influence on Cm(III) chemistry under envisioned UNF reprocessing solvent system conditions is expected to be significant based on the high concentration of this radical being generated.

Conclusions

Insight into the importance of the radiation-induced redox chemistry of Cm(III) in aqueous solution has been obtained from measured absolute rate coefficients for the reaction of Cm(III) with key radicals (e_{aq}^{-}, $^{\bullet}$H, $^{\bullet}$OH, and $NO_3^{\bullet}$) generated by pulsed electron radiolysis of acidic aqueous media.

These values, $k(e_{aq}^{-}) = (1.25 \pm 0.03) \times 10^{10}$ M^{-1} s^{-1}, $k(^{\bullet}H) = (5.16 \pm 0.37) \times 10^{8}$ M^{-1} s^{-1}, $k(^{\bullet}OH) = (1.69 \pm 0.24) \times 10^{9}$ M^{-1} s^{-1}, and k $(NO_3^{\bullet}) = (4.83 \pm 0.09) \times 10^{7}$ M^{-1} s^{-1}, suggest: (i) oxidation of Cm(III) by the $^{\bullet}OH/NO_3^{\bullet}$ radical to produce a transient Cm(IV) species could occur readily under anticipated reprocessing conditions, and thus propagate radiolysis in ligands that would normally be outside of either instigating radical's redox potential, i.e., E^{o} >2.7 V; and (ii) reduction of Cm(III) may also happen in other aqueous solutions typically used for the manipulation of Cm(III), e.g., $HClO_4$, where $e_{aq}^{-}/^{\bullet}H$ are not as effectively scavenged as in HNO_3, and thus Cm(II) may also facilitate more extensive radiolysis.

Overall, the presented kinetic data indicate that a steady-state concentration, albeit very low, of Cm(II) and Cm(IV) could exist in irradiated aqueous solutions and be available to undergo subsequent redox chemistry with other solutes (e.g. ligands and other metal ions). This is particularly plausible as their natural half-lives ($\tau_{1/2}$ ~ 12 and 20 μs, respectively)[21] are comparable if not greater than their instigating radicals, all of which are well known to propagate radiolysis.[27,52]

Conflicts of interest

There are no conflicts to declare.

Acknowledgements

Reported experiments were funded by the Laboratory Directed Research and Development Program, U.S. Department of Energy (DOE), under DOE Idaho Operations Office contract DEAC07-05ID14517 with Idaho National Laboratory. Data analysis and manuscript preparation was supported by the U.S. Department of Energy, Office of Science, Office of Basic Energy Sciences, under Award DE-SC0021372. Mezyk was supported by a Nuclear Energy Universities Program (NEUP) grant DE-NE0008406. The efforts of Cook and pulsed electron irradiation experiments at the Laser-Electron Accelerator Facility of the Brookhaven National Laboratory Accelerator Center for Energy Research were supported by the US-DOE Office of Basic Energy Sciences, Division of Chemical Sciences, Geosciences, and Biosciences under contract DE-SC0012704.

Notes and references

(1) Strategies and Considerations for the Back End of the Fuel Cycle, Nuclear Technology Development and Economics, NEA No. 7469, 2021.
(2) G.T. Seaborg, *Radiochim. Acta*, 1993, **61 (3-4)**, 115.
(3) S. Cotton, 2004. Comprehensive Coordination Chemistry II, McCleverty, J.A., Meyer, T.J. (Ed.) Elsevier, Oxford, vol. 3, pp. 93–188.
(4) C.J. Burns, M.P. Neu, H. Boukhalfa, K.E. Gutowski, NJ. Bridges, R.D. Rogers, 2004. Comprehensive Coordination Chemistry II, McCleverty, J.A., Meyer, T.J. (Ed.), Elsevier, Oxford, vol. 3, pp. 189–332.
(5) J.J. Katz, L.R. Morss, N.M. Edelstein, J. Fuger, 2006. The Chemistry of the Actinide and Transactinide Elements, Katz, J.J., Morss, L.R., Edelstein, N.M., Fuger, J. (Ed.), Springer, Dordrecht, vol. 1, pp. 1–17.
(6) G. Modolo, A. Wilden, A. Geist, D. Magnusson, and R.A. Malmbeck, *Radiochim. Acta*, 2012, **100**, 715.
(7) B. Moyer, G. Lumetta, B. Mincher, B., 2015. Minor Actinide Separation in the Reprocessing of Spent Nuclear Fuels: Recent Advances in the United States. Reprocessing and Recycling of Spent Nuclear Fuel; Taylor, R., Ed.; Woodhead Publishing: Oxford, UK, pp 289–312.
(8) K.L. Nash, *Solv. Extr. Ion Exch.*, 2015, **33 (1)**, 1.
(9) J. Veliscek-Carolan, *J. Hazard. Mater.*, 2016, **318**, 266.
(10) C.R. Heathman, T.S. Grimes, S. Jansone-Popova, A.S. Ivanov, V.S. Bryantsev, and P.R. Zalupski *Dalton Trans.*, 2018, **(47)**, 1092.
(11) T.S. Grimes, C.R. Heathman, S. Jansone-Popova, A.S. Ivanov, S. Roy, V.S. Bryantsev, and P.R. Zalupski, Inorg. Chem. 2018, **57 (3)**, 1373.
(12) A. Bhattacharyya, P. K. Mohapatra, *Radiochim. Acta*, 2019, **107 (9-11)**, 931.
(13) A. Geist, J.-M. Adnet, S. Bourg, C. Ekberg, H. Galan, P. Guilbaud, M. Miguirditchian, G. Modolo, C. Rhodes, R. Taylor, *Sep. Sci. Technol.*, 2020, DOI: 10.1080/01496395.2020.1795680.
(14) T.S. Grimes, C.R. Heathman, S. Jansone-Popova, A.S. Ivanov, V.S. Bryantsev, and P.R. Zalupski, *Inorg. Chem.* 2020, **59 (1)**, 138.
(15) B.J. Mincher, S.P. Mezyk, G. Elias, G.S. Groenewold, C.L. Riddle, and L.G. Olson, *Solvent Extr. Ion Exch.*, 2013, **31**, 715.
(16) B.J. Mincher, S.P. Mezyk, G. Elias, G.S. Groenewold, J.A. LaVerne, M. Nilsson, J. Pearson, N.C. Schmitt, R.D. Tillotson, and L.G. Olson, *Solvent Extr. Ion Exch.*, 2014, **32**, 167.
(17) C.A. Zarzana, G.S. Groenewold, B.J. Mincher, S.P. Mezyk, A. Wilden, H. Schmidt, G. Modolo, J.F. Wishart, and A.R. Cook, *Solvent Extr. Ion Exch.*, 2015, **33(5)**, 431.
(18) G.P. Horne, J.J. Kiddle, C.A. Zarzana, C. Rae, J.R. Peller, A.R. Cook, S.P. Mezyk, and B.J. Mincher, *Dalton Transactions*, 2019, **48**, 11547.
(19) G.P. Horne, C.A. Zarzana, C. Rae, A.R. Cook, S.P. Mezyk, P.R. Zalupski, A. Wilden, and B.J. Mincher, *Physical Chemistry Chemical Physics*, 2020, **22**, 24978.
(20) T. Toigawa, D.R. Peterman, D.S. Meeker, T.S. Grimes, P.R. Zalupski, S.P. Mezyk, A.R. Cook, S. Yamashita, Y. Kumagai, T. Matsumura, and G.P. Horne, *Physical Chemistry Chemical Physics*, 2021, **23**, 1343.
(21) S. Gordon, J.C. Sullivan, and A.B. Ross, *J. Phys. Chem. Ref. Data*, 1986, **15 (4)**, 1357.
(22) A.K. Pikaev, A.V. Gogolev, V.P. Shilov, and A.M. Fedoseev, *Isotopenpraxis Isotopes in Environmental and Health Studies*, 1990, **26 (10)**, 465.
(23) B.J. Mincher and S.P. Mezyk, *Radiochim. Acta*, 2009, **97**, 519.
(24) G.P. Horne, T.S. Grimes, B.J. Mincher, and S.P. Mezyk, *J. Phys. Chem. B*, 2016, **120 (49)**, 12643.
(25) T.S. Grimes, G.P. Horne, C.J. Dares, S.M. Pimblott, S.P. Mezyk, and B.J. Mincher, *Inorganic Chemistry*, 2017, **56 (14)**, 8295.
(26) G.P. Horne, T.S. Grimes, W.F. Bauer, C.J. Dares, S.M. Pimblott,

S.P. Mezyk, and B.J. Mincher, *Inorganic Chemistry*, 2019, **58**, 8551.

(27) G. V. Buxton, C. L. Greenstock, W. P. Helman and A. B. Ross, *J. Phys. Chem. Ref. Data*, 1988, **17**, 513.

(28) Y. Katsumura, The Chemistry of Free Radicals: N-Centered Radicals, John Wiley & Sons, Chichester, 1998.

(29) N.E. Bibler, *J. Phys. Chem.*, 1974, **78 (3)**, 211.

(30) D.T. Reed, D.L. Bowers, *Radiochim. Acta*, 1990, **51**, 119.

(31) D. Magnusson, B. Christiansen, R. Malmbeck, and J.-P. Glatz, *Radiochim. Acta*, 2009, **97**, 497.

(32) S.P. Mezyk, B.J. Mincher, C. Ekberg, and G. Skarnemark, *J. Radioanal. Nucl. Chem.*, 2013, **296**, 711.

(33) L.R. Morss, Comparative Thermochemical and oxidation-reduction properties of lanthanides and actinides., in Handbook on the Physics and Chemistry of Rare Earths, Col 18: Lanthanide/Actinides: Chemistry, Chapter 122, Eds.. Gschneidner,, K.A. Jr.; Eyring, L.; Chopin, G.R.; Lander, G.H., Elsevier Science, B.V., 1994.

(34) J.C. Sullivan, S. Gordon, W.A. Mulac, K.H. Schmidt, D. Cohen, and R. Sjoblom, *Inorg. Nucl. Chem. Let.*, 1976, **12**, 599.

(35) V.P. Shilov, *Radiokhimiya*, 1994, **35(3)**, 255.

(36) H.-U. Zwicky, J. Low, and E. Ekeroth, Technical Report: Svensk Kaernbraenslehantering AB, (TR-11-03), 2011 1.

(37) M. Struzbecher-Hoehne, C. Goujon, G.J.P. Deblonde, A.B. Mason, and R.J. Abergel, *J. Am. Chem. Soc.*, 2013, **135**, 2676.

(38) P. Y. Jiang, Y. Katsumura, K. Ishigure and Y. Yoshida, *Inorg. Chem.*, 1992, **31**, 5135.

(39) G. Garaix, G.P. Horne, L. Venault, P. Moisy, S.M. Pimblott, J.-L. Marignier, and M. Mostafavi, *J. Phys. Chem. B*, 2016, **120 (22)**, 5008.

(40) W.T. Carnall, P.R. Fields, D.C. Stewart, and T.K. Keenan, *J. Inorg. Nucl. Chem*, 1958, **6**, 213.

(41) J. F. Wishart, A. R. Cook, and J. R. Miller, *Review of Scientific Instruments*, 2004, **75 (11)**, 4359.

(42) G.V. Buxton and C.R. Stuart, *J. Chem. Soc. Faraday Trans.*, 1995, **92**, 279.

(43) A.K. Pikaev, V.P. Shilov, and A.V. Gogolev, *Russ. Chem. Rev.*, 1997, **66(9)**, 763.

(44) N.B. Mikheev, M.Z. Kazakevich, and I.A. Rumer, *Radiochem.*, 1992, **34**, 293.

(45) S.M. Pimblott and J.A. LaVerne, *J. Phys. Chem. A*, 1998, **102**, 2967.

(46) G. Hug, Optical Spectra for Nonmetallic Inorganic Transient Species in Aqueous Solution, NSRDS-NBS 69, US Department of Commerce, National Bureau of Standards, 1981.

(47) A.G. Crof, *Nuclear Technology*, 1983, **62**, 335.

(48) P.K. Khopar and J.N. Mathur, *J. Inorg. Nucl. Chem.*, 1974, **36**, 3819.

(49) P.K. Khopar and J.N. Mathur, *Thermochim. Acta.*, 1980, **37**, 71.

(50) T.K. Keenan, *J. Am. Chem. Soc.*, 1961, **83**, 3719.

(51) C. Keller, The Chemistry of the Transuranium Elements, Verlag Chemie, Weinheim, 1971.

(52) S.P. Mezyk, T.D. Cullen, K.A. Rickman, and B.J. Mincher, *Int. J. Chem. Kin., 2017*, **49 (9)**, 635.